Analytica Chimica Acta 1191 (2022) 339289

Contents lists available at ScienceDirect

Analytica Chimica Acta

journal homepage: www.elsevier.com/locate/aca

SERS-based boronate affinity biosensor with biomimetic specificity and versatility: Surface-imprinted magnetic polymers as recognition elements to detect glycoproteins

Cunming Hu [a], Fei Peng [a], Fang Mi [a], Ying Wang [a], Pengfei Geng [a], Lin Pang [a], Yuhua Ma [a], Guixin Li [a], Yingjun Li [b], Ming Guan [a, *]

[a] College of Chemistry and Chemical Engineering, Xinjiang Normal University, Urumqi, 830054, China
[b] College of Foreign Languages, Xinjiang Normal University, Urumqi, 830054, China

HIGHLIGHTS

- Boronic acid modified core-shell Au-MPBA@Ag exhibit high SERS activity.
- Controllable-oriented surface imprinting increases the utilization of binding sites.
- MMIPs can be easily separated by an external magnetic field.
- The proposed method exhibits both biomimetic specificity and versatility.
- The detection limit of this SERS sensor for HRP was 0.053 ng/mL.

GRAPHICAL ABSTRACT

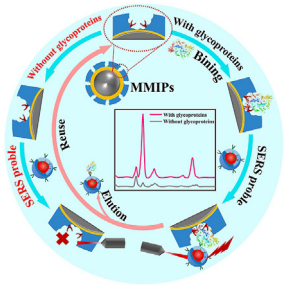

ARTICLE INFO

Article history:
Received 7 July 2021
Received in revised form
12 November 2021
Accepted 15 November 2021
Available online 17 November 2021

Keywords:
Boronate affinity
SERS
Magnetic molecularly imprinted polymer
Glycoprotein
Controllable-oriented surface imprinting

ABSTRACT

Glycoproteins are a class of proteins with significant biological functions and clinical implications. Due to glycoproteins' reliability for the quantitative analysis, they have been used as biomarkers and therapeutic targets for disease diagnosis. We propose a sandwich structure-based boronate affinity biosensor that can separate and detect target glycoproteins by magnetic separation and Surface-enhanced Raman scattering (SERS) probes. The biosensor relies on boronic acid affinity magnetic molecularly imprinted polymer (MMIPs) with pH response as "capturing probe" for glycoproteins, and Au-MPBA@Ag modified with 4-mercaptophenylboronic acid (MPBA) as SERS probes, among which, MPBA has both strong SERS activity and can specifically recognize and bind to glycoproteins. MMIPs ensured specific and rapid analysis, and SERS detection provided high sensitivity. The proposed boronate affinity SERS strategy exhibited universal applicability and provided high sensitivity with limit of detection of 0.053 ng/mL and 0.078 ng/mL for horseradish peroxidase and acid phosphatase, respectively. Ultimately, the boronate affinity SERS strategy was successfully applied in detection of glycoprotein in spiked serum sample with recovery between 90.6% and 103.4%, respectively. In addition, this study used a portable Raman meter, which can meet the requirements of point-of-care testing. The biosensor presented here also has advantages in terms of cost-effectiveness, stability, and detection speed.

* Corresponding author.
E-mail address: 635880760@qq.com (M. Guan).

https://doi.org/10.1016/j.aca.2021.339289
0003-2670/

1. Introduction

As one of the essential products of protein glycosylation, glycoproteins usually appear as enzymes or signaling molecules and play crucial roles in many biological processes, such as molecular recognition, immune response, and inflammation [1,2]. Glycoproteins contain more than 50% of total proteins in mammalian systems, and their abnormal structural changes and expression are associated with the occurrence and development of several diseases [3]. For example, Acid phosphatase (ACP) is a glycoprotein that plays a vital role in phosphatase clearance. Abnormal elevation of ACP in human being is related to prostate cancer and other venous, renal, and skeletal-related disorders [4,5]. Therefore, developing a convenient method for detecting glycoproteins is an urgent issue.

Currently, several methods have been used for the analysis of glycoproteins, including lectin affinity assay [6,7], hydrazide chemistry [8,9], hydrophilic chromatography [10,11], and immunoassays [12,13]. However, those methods can not be widely employed due to being sophisticated, time-consuming, expensive, unstable, and low selectivity. It is more challenging to identify trace glycoproteins directly using those methods. Recently, boronate affinity materials have attracted much attention on the utilization for glycoproteins enrichment [14–16]. This application is based on the fact that boronic acids can covalently interact with cis-diol-containing glycoproteins to form stable cyclic esters in basic environments and reversibly undergo the backward reaction under acidic conditions [17,18]. However, boronate affinity materials still have two limitations: 1) they cannot recognize specific cis-diol-containing glycoproteins due to class selectivity [17,19]; 2) most materials have a poor affinity, with dissociation constants ranging from 10^{-1}–10^{-3} M [20]. Therefore, low concentration of glycoproteins is poorly captured by traditional boronate affinity materials. Thus, it is essential to develop new boronate functionalized materials with strong binding ability and high selectivity.

Molecularly imprinted polymers (MIPs) open a new door for highly efficient separation and enrichment of target analytes in complex matrices [21–23]. They are synthesized by the copolymerization of functionalized monomers in the presence of a template and exhibit affinity and specificity for target molecules [24,25]. In comparison to antibodies, MIPs are easy to prepare, less expensive to produce, and more stable. Therefore, MIPs have been widely used in catalysis [26], sensing [27], separation [28], and disease diagnosis [29]. Recently, surface imprinted polymers with boronic acid affinity materials as cores for the adsorption of glycoproteins have been widely reported [30,31]. The boronic acid group's class selectivity toward template glycoproteins and the fact that MIPs can create imprinting cavities that match the template molecules makes boronate affinity MIPs exhibit excellent specificity, high affinity, and excellent anti-interference properties [32]. Since time consumption is also key to glycoprotein pretreatment, candidates must be rapidly separated. Magnetic nanoparticles have attracted much attention because of their high specific surface area and rapid separation under a certain strong magnetic field [33–35]. Therefore, many boronate affinity magnetic molecularly imprinted polymers (MMIPs) are prepared for rapid enrichment separation of trace glycoproteins in complex matrices [14,21,36,37].

Surface-enhanced Raman scattering (SERS) has been widely used in the detection of various pathogens and biomarkers due to its excellent photostability, ultra-high sensitivity, rapid readout, and point-of-care testing (POCT) [38,39]. Furthermore, the use of SERS tags dramatically expands the application scope of this advanced method. In previous work, SERS tags (Au-reporter@Ag) prepared by embedding a Raman reporter molecule between a gold core silver shell achieved highly sensitive detection of cardiac infarction biomarkers as well as psychoactive drugs [40,41]. However, due to the sensitivity of SERS sensor processing, SERS signals are prone to be disturbed in complex matrices. Interestingly, the combination of MIPs and SERS can make up for the defects existing in SERS detection mentioned above. A "sandwich-type" boronic acid affinity SERS sensor was first developed by Liu et al. [42]. The sensor relies on a sandwich structure formed by boronic acid affinity MIPs, target glycoproteins, and boronic acid affinity SERS probes. Similarly, Li and co-workers [43] utilized a SERS sensor based on boronic acid affinity MIPs array recognition for highly selective detection of ACP with LOD was 0.1 ng/mL. Although the above methods achieve highly selective detection of target glycoproteins, they cannot be used for POCT. For example, using MIPs arrays to capture glycoproteins requires multiple steps such as elution interferents, drying, etc., which increases the detection time. Moreover, the Raman signal of the SERS tags was low and the Raman reporter molecules were vulnerable to interference of the environment. POCT is widely used in clinical diagnosis because of its easy operation, rapidity, and miniaturization of experimental instruments [44]. To further explore this field, we performed imprinting of glycoproteins on the surface of boronic acid functionalized magnetic nanoparticles, which can selectively adsorb targets in the analytical liquid and enrich separation under an external magnetic field. Furthermore, SERS probes with strong Raman signals were prepared to meet the threshold of portable Raman instrument POCT.

Herein, we established a boronate affinity sandwich strategy based on MMIPs and SERS for specific recognition and highly sensitive detection of trace amounts of glycoproteins in complex samples. The boronate affinity MMIPs secured the specificity and the SERS detection promoted the sensitivity. Since 4-mercaptophenylboronic acid (MPBA) not only has strong SERS activity but also can specifically recognize and bind to glycoproteins [45]. Therefore, MPBA was firstly embedded between gold core and silver shell, and the obtained core-shell nanoparticles (Au-MPBA@Ag) had strong Raman signals. Since the Raman reporter molecule is between the gold core and silver shell, the SERS signal is hard to be affected by the environment and has good stability and repeatability. Then the above nanoparticles were functionalized with MPBA to obtain SERS probes that could label glycoproteins. Moreover, the whole analysis process was carried out in solution, which shortens the analysis time and avoids low efficiency of the reaction at the liquid/solid interface. Analysis of multiple glycoproteins (such as horseradish peroxidase (HRP), transferrin (TRF), and ACP) showed that the synthesized MMIPs demonstrated the specific recognition of target glycoproteins, indicating the general applicability of the method. Ultimately, the practicality of their biological applications were further evaluated by quantitative analysis of HRP, ACP, and TRF in serum.

2. Experimental section

Details of reagents, materials, and instruments are provided in the electronic supporting information (ESI).

2.1. Preparation of SERS probes

The SERS probe was prepared in three steps: 1) The Raman reporter was bonded to the surface of gold nanoparticles by Au–S bond; 2) The reduction of Ag^{+} to Ag was wrapped onto the surface of the above particles to form a core-shell structure; 3) The

above core-shell nanoparticles were functionalized with boronic acid. See ESI for preparation details.

2.2. Preparation of boronic acid modified magnetic nanoparticles

The amino group modified magnetic nanoparticles (Fe_3O_4—NH_2) were prepared according to a previously reported method with slight modifications [46]. 2.0 g of $FeCl_3 \cdot 6H_2O$, 13.0 g of 1,6-hexanediamine, 4.0 g of NaAc, 1.0 g of polyethylene glycol were added to 60 mL of ethylene glycol, dissolved by stirring and placed in a 100 mL Teflon lined autoclave to react at 198 °C for 8 h. Then the obtained Fe_3O_4—NH_2 was collected under magnetic field and rinsed sequentially with water and ethanol for three times. Finally, it was dried under a vacuum at 50 °C overnight.

Fe_3O_4—NH_2 was boronic acid functionalized for immobilization of glycoproteins. First, 200 mg of 4-formylphenylboronic acid (FPBA) and 250 mg of $NaBH_3CN$ were dissolved in 50 mL of methanol, then 100 mg of Fe_3O_4—NH_2 was dispersed into the above solution and sonicated for 20 min. The obtained homogeneous solution was stirred at room temperature for 24 h. The products were collected by a magnet and washed with methanol and water several times, dried in a vacuum at 60 °C for 12 h, and the obtained products were denoted as FPBA-MNPs.

2.3. Immobilization of glycoproteins

50 mg FPBA-MNPs were dispersed into 50 mL of PBS (0.1 M phosphate buffer solution, pH 7.4) by sonication, then 15 mg of HRP was added and fixed by stirring at 25 °C for 1 h. Finally, rinsed with PBS until there was no UV—Vis absorption at 214 nm in the solution.

2.4. Controllable-oriented surface imprinting of glycoproteins

In a 500 mL round bottom flask, the above glycoprotein immobilized magnetic particles were ultrasonic completely dispersed in 150 mL absolute ethanol containing 2.8 mL ammonia. Then 50 mL of absolute ethanol (containing 100 μL TEOS) was added and the mixture was stirred at room temperature for some time. By controlling the hydrolysis time of TEOS, the thickness of the MMIPs layer was optimized, HRP-imprinted MNPs were finally collected by a magnet and washed with ethanol several times and dried at 50 °C under vacuum overnight. Then, the template HRP was removed by washing with 0.1 M acetic acid solution containing 10% SDS. Finally, MMIPs were collected by magnetic separation, washed with ethanol and deionized water several times, and dried at 50 °C overnight.

Magnetic non-imprinted nanoparticles (MNIPs) were prepared using the same procedure except without a complete glycoprotein immobilization step. The resulting MNIPs were FPBA-MNPs covered by a layer of silica shell with the same thickness as the glycoprotein imprinted MNPs. ACP-imprinted MNPs and TRF-imprinted MNPs were prepared by replacing the HRP stock solution with the same ACP and TRF solution volume. All steps were the same except that the imprinting time was optimized.

2.5. Sample preparation and practical application for HRP, ACP and TRF assay

The target glycoproteins were dissolved in PBS (pH 7.4) to make up a stock solution with a concentration of 10 mg/mL and diluted with the above PBS to the desired concentration and then stored at 4 °C before use. Fetal bovine serum thawing was followed by a 100-fold dilution with PBS, and a certain concentration of HRP was added to prepare the spiked samples. To evaluate the versatility, the proposed method was applied in quantitative detection of ACP and TRF from spiked serum samples. Human serum was supplied by healthy volunteers. Some necessary processes were conducted to remove large molecules and proteins to get the serum samples. The blood samples were segregated by adding acetonitrile and centrifuged at 12,000 rpm for 5 min after stored for 2 h at 25 °C. Then, the supernatant serum samples were 1000-fold diluted with PBS before analysis, and a certain concentration of ACP was added to prepare the spiked samples. Since TRF are relatively more abundant in serum, supernatant serum samples were 10^6-fold diluted with PBS before analysis, and a certain concentration of TRF was added to prepare the spiked samples. For comparison, the ACP and TRF from human serum samples were also determined by a commercial ELISA kit according to manufacturer's instructions.

2.6. SERS detection of target glycoproteins

In small test cups, 0.2 mg MMIPs were dispersed in 1 mL target protein standard solution (or real sample solution), and the mixture was shocked for 30 min. Then the MMIPs with adsorbed glycoproteins were collected by an external magnet, washed with PBS (pH 7.4) to remove excess proteins, and then added 200 μL SERS probes to label the glycoproteins captured by MMIPs. After incubation for 8 min, the excess SERS probes were washed with acetonitrile: 0.01 M pH 9.0 PBS (30:70, v/v). Finally, the MMIPs-glycoproteins-SERS probes sandwich conjugate were resuspended in 200 μL PBS (pH 7.4), shaken gently to complete dispersion. For quantitative analysis, the small test cup was placed on the detection holder and analyzed by a portable Raman spectrometer. Raman spectra were recorded with a 785 nm laser at 200 mW power with an integration time of 500 ms and accumulated three times. All Raman spectra were averages of 5 repeated measurements and were baseline corrected.

3. Results and discussion

3.1. Principle of SERS-based biosensor for detection of target glycoproteins

The construction of the SERS-based boronic acid affinity sandwich method and the principle of detecting target glycoproteins are shown in Fig. 1. Fig. 1A and **B** shows the fabrication procedures of boronic acid affinity MMIPs and boronic acid functionalized SERS probes, respectively. Fig. 1C indicates that the boronate affinity SERS strategy for detecting target glycoproteins is based on forming the sandwich structure of boronate affinity MMIPs - target glycoproteins - SERS probes. SERS analysis relies on boronic acid affinity MMIPs that are functionally analogous to capture antibodies and Au-MPBA@Ag modified with MPBA as SERS probes. First, the target glycoproteins in the sample are specifically captured by the MMIPs, and the presence of Fe_3O_4 causes the magnetic separation of glycoproteins from the complex matrix. Subsequently, the SERS probe was added and incubated to form a sandwich structure. Finally, the sandwich structure was collected by magnetic separation and the SERS signal was measured with a portable Raman meter.

3.2. Optimization of the method

In order to make the SERS-based boronate affinity sandwich strategy quantitative for the target glycoproteins under the optimal conditions, some parameters were optimized. The experimental conditions that showed the best results were as follows: 1) During

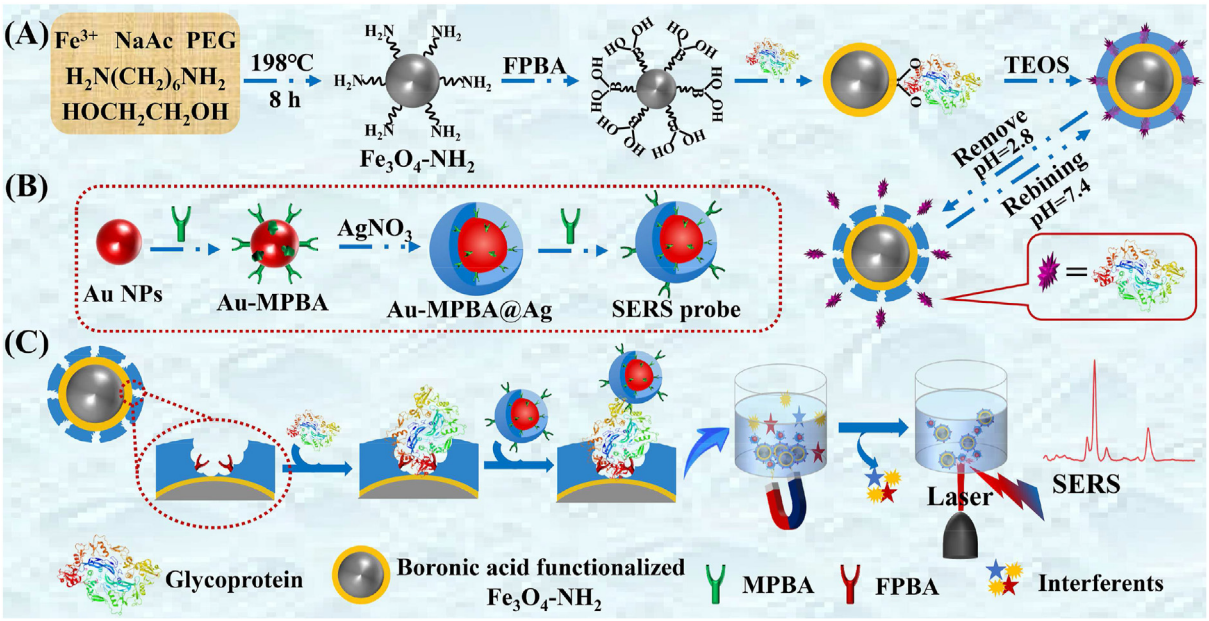

Fig. 1. Principle of SERS-based boronate affinity sandwich assay for detection of target glycoproteins. (A) The preparation procedure of boronate affinity MMIPs. (B) The preparation procedure of boronic acid functionalized SERS probes. (C) Schematic of sandwich assay construction and detection of target glycoproteins.

the preparation of the SERS probes, the volume of 1 mM of MPBA in the Au-MPBA@Ag core-shell nanoparticles was 200 μL (Fig. S1); the reaction time between AuNPs and MPBA was 15 min (Fig. S2); the volume of 20 mM of $AgNO_3$ in Au-MPBA@Ag was 100 μL (Fig. S3). 2) The optimal incubation time between the target glycoprotein and the boronic acid functionalized SERS probes was 8 min (Fig. S4). 3) During the preparation of MMIPs, the concentration of HRP was 0.3 mg/mL (Fig. S5), the imprinting time was 70 min (Fig. S6), and the optimal elution time of template was 60 min (Fig. S7). 4) The affinity time of MMIPs to capture target glycoproteins was 30 min, and the optimal pH was 7.4 (Figs. S8 and S9). 5) The excess SERS probes in the sandwich structure of MMIPs-glycoprotein-SERS probes were washed with acetonitrile: 0.01 M pH 9.0 PBS (30:70, v/v) (Table S1).

3.3. Characterization of boronic acid functionalized SERS probes

The design and fabrication of boronic acid modified SERS probes mainly involve attaching the Raman reporter MPBA to the surface of AuNPs, followed by a layer of silver shell covered on the surface, and further modification with MPBA. First, the nanoparticles were characterized by TEM. Fig. 2A shows that AuNPs were well distributed with a size of about 16 nm (Fig. 2C). Fig. 2B is the TEM of the SERS probe, which has an obvious core-shell structure with relatively uniform size and an average size of about 33 nm (Fig. 2C). UV–Vis spectra of different nanoparticles, as shown in Fig. 2E, demonstrates a red-shift for Au-MPBA (525 nm) from AuNPs (520 nm). The change results from the conjugation effect of the introduced MPBA, indicating that Au-MPBA was synthesized successfully. When Ag^+ was reduced into silver shell, the absorption peak of AuNPs disappeared and the characteristic absorption peak of silver appeared at 400 nm, indicating that the surface of gold core was covered by silver. The small red-shift of the absorption peak of the formed SERS probes after modification by boronic acid gives a preliminary indication of success. Meanwhile, it was also proved by the EDS analysis of the SERS probe (Fig. 2D). The characteristic elements Au, Ag and S in the SERS probe appeared in the EDS spectra, in which, the S element was provided by MPBA. Furthermore, the SERS probe was employed to label the target glycoprotein simultaneously with Au-MPBA@Ag. Since there is no boronic acid on the Ag that binds glycoproteins, the conjugate does not produce any signal, while the SERS probe does the opposite (Fig. S11).

The AgNPs with higher SERS activity had uneven particle size, leading to unstable SERS enhancement, while the SERS activity of AuNPs with uniform distribution was low. Au@Ag core-shell nanoparticles with two metals have high and stable SERS activity. Therefore, we synthesized Au-MPBA, Ag-MPBA, and Au@Ag-MPBA by reference (see ESI for experimental details), and along with Au-MPBA@Ag synthesized in this study. Their Raman enhancement activities were evaluated under the same measurement parameters. It can be seen from Fig. S12 that Au-MPBA exhibits the weakest SERS signal among these different types of nanoparticles. Both Au@Ag-MPBA and Au-MPBA@Ag with gold core silver shell structure, the Raman signals differed by nearly three times; this is due to intercalation of Raman reporter molecules into the crevices of the core-shell which creates a "hot spot" structure with a stronger local plasmon resonance effect under the synergistic effect of bimetallic. Similarly, the SERS signals of different nanoparticles were compared in the synthesis of SERS probes (Fig. 2F). The pure AuNPs did not have any SERS signal, and only a weak SERS signal was exhibited after the surface was conjugated with MPBA. The SERS signal increased sharply when a layer of the silver shell was attached to the above particles' surface. The SERS signal increased a little after boronic acid modification. Therefore, the strong Raman signal of the SERS probe lays the foundation for the ultrasensitive detection of glycoproteins. Raman signal acquisition was performed for the prepared nine batches of core-shell SERS probes, and the RSD of the SERS signal at the characteristic peak 1078 cm^{-1} was only 4.29%. Moreover, the SERS probes were stable for at least 30 days in the dark at 4 °C, indicating that the core-shell SERS probes have good repeatability and stability (Figs. S13 and S14).

3.4. Characterization of HRP-imprinted MNPs

Design and preparation of MMIPs, mainly included synthesis of amino-modified Fe_3O_4 NPs, functionalization of boronic acids,

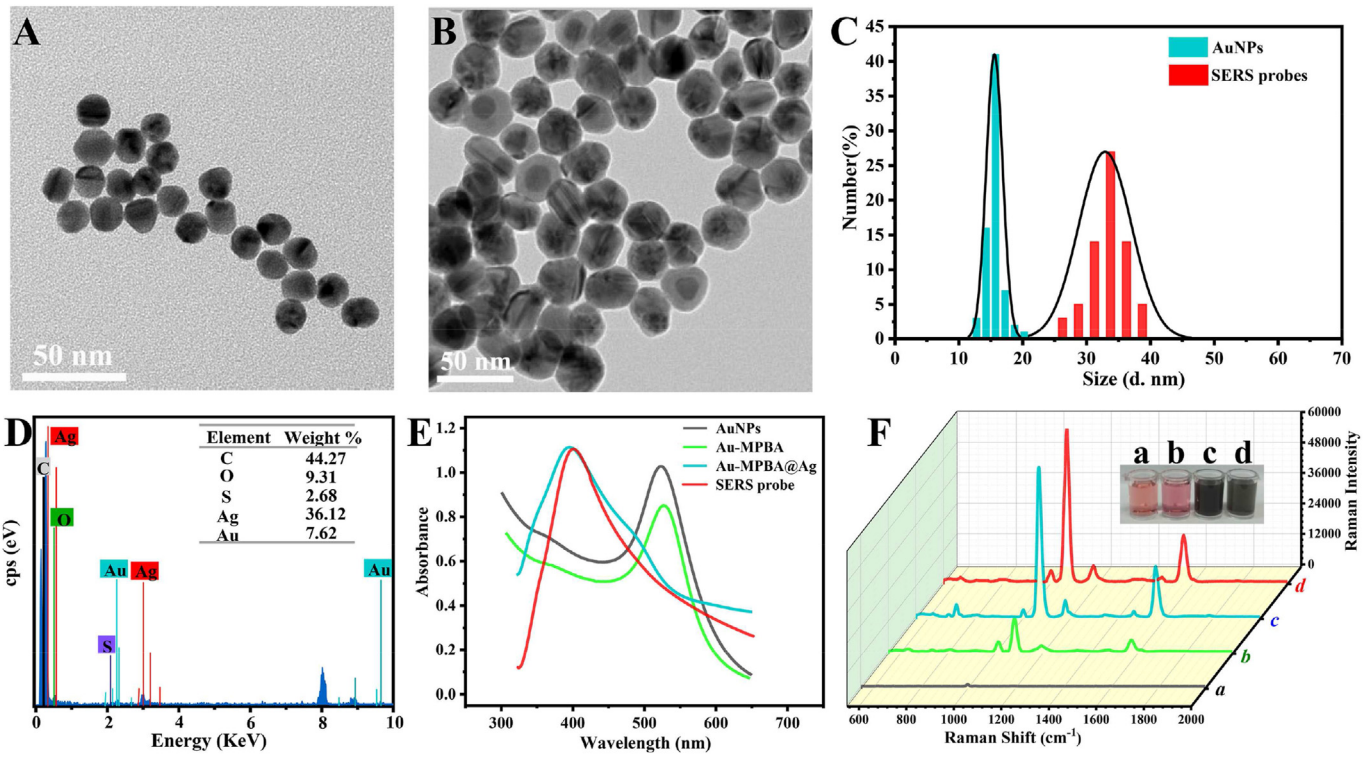

Fig. 2. TEM of (A) AuNPs and (B)SERS probes. (C) Particle size distribution of AuNPs and SERS probes. (D) EDS of the SERS probe. (E) UV–Vis spectra of AuNPs, Au-MPBA, Au-MPBA@Ag and SERS probes. (F) SERS spectra of a: AuNPs, b: Au-MPBA, c: Au-MPBA@Ag and d: SERS probes. The inset shows the color of corresponding nanoparticles. (For interpretation of the references to color in this figure legend, the reader is referred to the Web version of this article.)

anchoring of glycoproteins, and thickness controllable imprinting. For morphology measurements, the shape and size of Fe_3O_4–NH_2 and MMIPs were studied by TEM. Fig. 3A shows that Fe_3O_4–NH_2 were successfully prepared by a one-pot solvothermal reduction method with their average diameter at around 134 nm. As shown in Fig. 3B and C, MMIPs had an obvious core-shell structure with an average diameter of about 158 nm, significantly larger than that of Fe_3O_4–NH_2, confirming the formation of a silica film on Fe_3O_4–NH_2. TEM of MNIPs also revealed an obvious core-shell structure with a particle size of about 160 nm (Fig. 3D). The morphology of the MNIPs was similar to the MMIPs, indicating that template protein displayed little influence on the morphology. The measuring magnetization curves of Fe_3O_4–NH_2, FPBA-MNPs and MMIPs using VSM are shown in Fig. 3G. All materials showed good magnetic, in which the magnetic saturation (MS) value of Fe_3O_4–NH_2 was 77.85 emu/g and it showed a small decrease after boronic acid functionalization (75.87 emu/g). Compared with Fe_3O_4–NH_2, the MS value of MMIPs decreased obviously, which was related to the surface covered with a layer of SiO_2. Moreover, the inset of Fig. 3G shows that the MMIPs could be adsorbed on the side of the vial within 20s when an external magnet was placed next to the vial, which further confirmed the strong magnetic response of MMIPs, and analytes can be easily separated from the mixture under an external magnetic field.

FT-IR was used to investigate the chemical structure of Fe_3O_4–NH_2, FPBA-MNPs and MMIPs. As shown in Fig. 3E, the spectrum of Fe_3O_4–NH_2 nanoparticles showed the signals at 581 cm^{-1} (Fe–O groups), 3410 cm^{-1} (N–H stretching vibration), 2926 and 2853 cm^{-1} (C–H stretching vibration of alkyl chains), indicating that 1,6-hexanediamine had been successfully modified on the surface of Fe_3O_4 NPs [47]. The spectrum of FPBA-MNPs showed characteristic absorption peaks at 1403 and 1516 cm^{-1}, corresponding to B–O adsorption bonds, indicating that FPBA had been grafted onto the surface of Fe_3O_4–NH_2 [48]. Compared to the spectrum of FPBA-MNPs, the absorption peak of MMIPs at 1124 cm^{-1} belonged to the stretching vibration of Si–O–Si [30]. The results confirmed that silica had been successfully wrapped on the surface of magnetic nanoparticles. To further determine the modification of Fe_3O_4–NH_2 surface by FPBA, elemental analysis of FPBA-MNPs was carried out using XPS. As shown in Fig. 3F, the N1s peak at 399.1 eV indicated that 1,6 - hexanediamine had been immobilized on the surface of magnetic nanoparticles. Due to the low B abundance, a weaker B1s peak appeared at 191.4 eV, indicating that FPBA had been immobilized on the surface of Fe_3O_4–NH_2. The crystal phases of Fe_3O_4–NH_2, FPBA-MNPs and MMIPs were identified by XRD analysis. As shown in Fig. 3H, XRD of the prepared materials showed the characteristic diffraction peaks of Fe_3O_4, and six characteristic diffraction peaks at $2\theta = 30.1°$, 35.4°, 43.2°, 53.4°, 57.1° and 62.5° can be indexed to (220), (311), (400), (422), (511) and (440), respectively, (JCPDS Card: 19–0629). This information indicates that the crystal structure of magnetite largely remained unchanged during the synthesis. Moreover, XRD of MMIPs exhibits the identical peak position as that of Fe_3O_4–NH_2 but with the peak intensity decreases, which confirmed that a layer of film material was imprinted on the surface of Fe_3O_4–NH_2.

The binding isotherm of the HRP-imprinted MNPs toward HRP was evaluated. As shown in Fig. 3I, the HRP-imprinted MNPs exhibited much stronger affinity toward HRP with an adsorption capacity of 43.8 mg/g compared to the non-imprinted MNPs. Scatchard plot analysis **(Fig. S15)** provided a dissociation constant (K_d) of $(7.11 \pm 0.43) \times 10^{-6}$ at pH 7.4. The strong binding strength of the prepared MMIPs favors the extraction of target HRP at a low

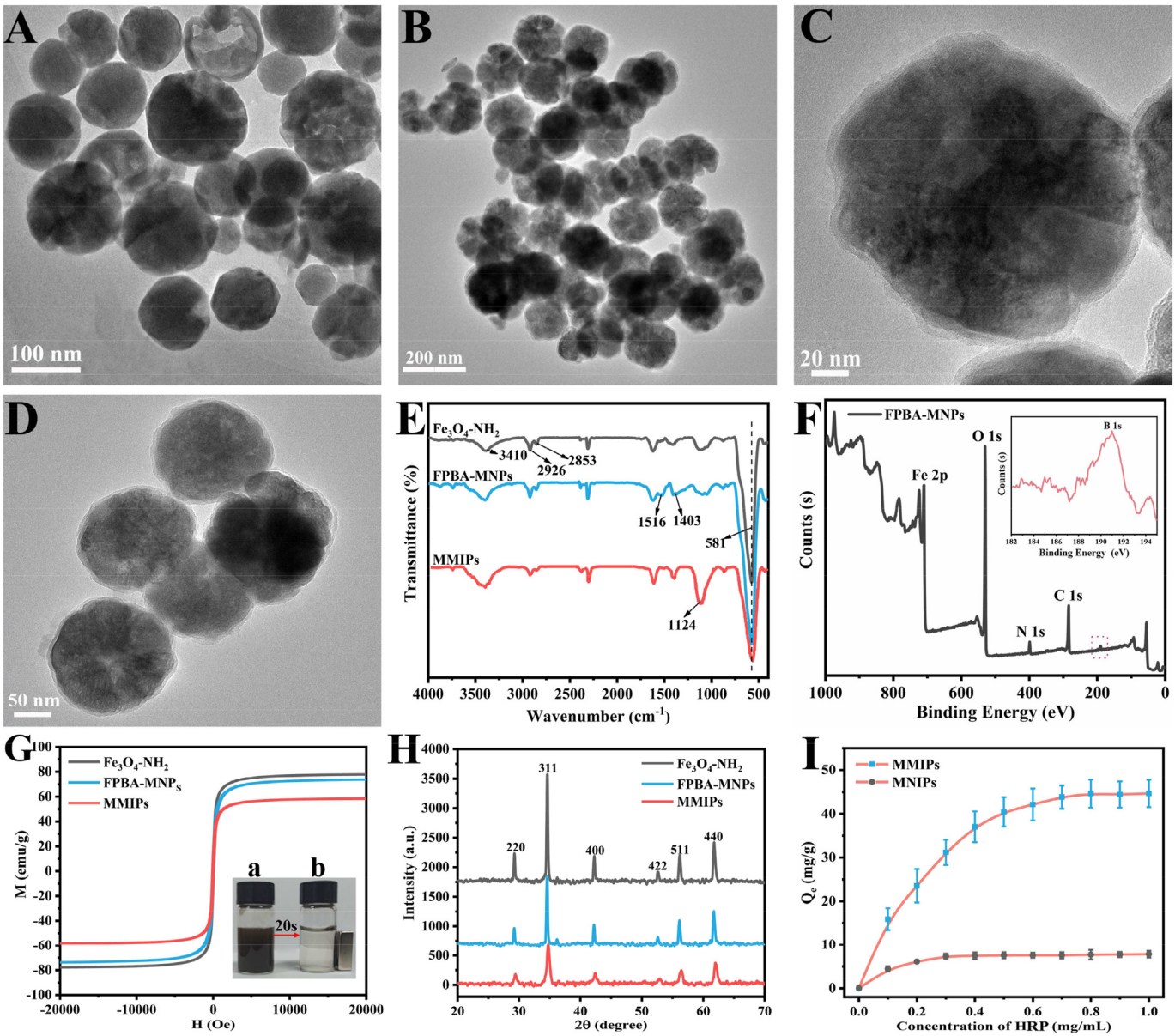

Fig. 3. TEM of (A) Fe_3O_4—NH_2, (B) MMIPs, and (D) MNIPs. (C) High magnification TEM of MMIPs. (E) FT-IR spectra and (H) XRD spectra of Fe_3O_4—NH_2, FPBA-MNPs and MMIPs. (F) XPS spectra of FPBA-MNPs. (G) The hysteresis curves of Fe_3O_4—NH_2, FPBA-MNPs and MMIPs, the inset is a photograph of the dispersion and magnetic separation of MMIPs. (I) Binding isotherms of MMIPs and MNIPs with HRP.

concentration. The imprinting efficiency was measured to be 42.8% (see the ESI), which means that, with 100 molecules of the template used for the imprinting, 42 template molecules provided well-imprinted cavities. Such a value is quite high in molecular imprinting, and therefore the imprinting approach was highly efficient.

3.5. Selectivity of the MMIPs-SERS biosensor

The SERS intensity of the FPBA-MNPs, MMIPs in the presence of several proteins, including HRP, TRF (a glycoprotein), ACP (a glycoprotein), AFP (a glycoprotein), BSA (a nonglycoprotein), and glucose were recorded under identical conditions to verify the selectivity of MMIPs. The concentration of HRP was 1000-fold lower than that of interfering proteins and glucose. The binding capacity of HRP, TRF, ACP and AFP on FPBA-MNPs was similar and much higher than that of BSA and glucose, as displayed in Fig. S16, confirming that boronic acid affinity materials had higher binding capacity for all glycoproteins. MMIPs exhibited a much higher response toward HRP than other glycoproteins, resulted from much higher binding capacity toward HRP (Fig. 4A). This remarkable selectivity can be attributed to the elimination of interference from other glycoproteins by the molecular imprinting technique. For template protein, there are recognition sites that match the size, shape, and functional groups of the template inside the imprinted polymers. For the MNIPs, there are no specific recognition sites for HRP so all the proteins were bound through the nonspecific binding affinity. So the SERS intensity did not displayed much difference. The cross-reactivity, estimated by the percentage of the SERS intensity of interfering protein over HRP, was employed to evaluate the selectivity of MMIPs to interfering proteins, as shown in Table S2. The molecular weight of OVA (44.3 kDa) is very close to

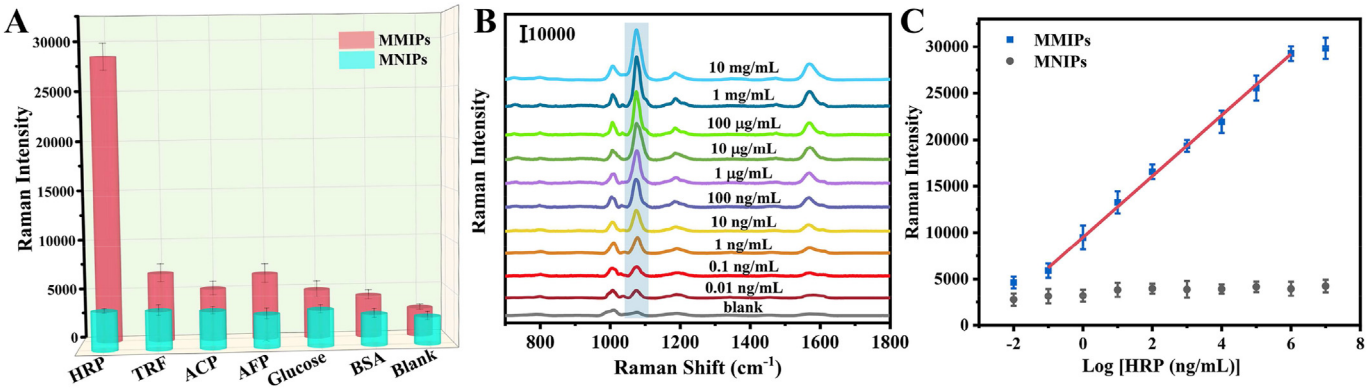

Fig. 4. (A) The selective recognition property of each compound with MMIPs and MNIPs. Sample: 1.0 μg/mL HRP or 1.0 mg/mL interfering substance. The blank sample contained no protein or glucose. (B) SERS spectra for HRP at different concentrations. (C) Calibration curve of SERS signal intensity at 1078 cm^{-1} for HRP at a concentration range of 0.01 ng/mL ~ 10 mg/mL. Error bars indicate the standard deviation of three replicate determinations.

that of HRP (44.2 kDa), resulted in the highest cross-reactivity of 9.1% and it was acceptable. Similarly, ACP-imprinted MNPs and TRF-imprinted MNPs showed good selectivity for template ACP and TRF, whereas their SERS intensities for other proteins glucose changed little compared with the blank sample (Fig. S19). These results benefited from the high specificity of boronate affinity MMIPs and the high efficiency of magnetic material separation, which was further guaranteed by boronate affinity SERS probes.

3.6. Method validation and universal applicability

Here, we examined the performance of the SERS sensor based on MMIPs recognition. HRP was used as a model glycoprotein. Under optimal conditions, the SERS spectra of HRP at a concentration of 0.01 ng/mL ~ 10 mg/mL are shown in Fig. 4B. It is not difficult to find that the SERS intensity increases with the increase of HRP concentration, and the characteristic peak at 1078 cm^{-1} for the quantitative detection of HRP in different concentration solutions. A response curve was obtained by plotting the SERS intensity at 1078 cm^{-1} against the logarithm of HRP concentration (Fig. 4C). The signal increased linearly with the logarithmic value of the target glycoprotein concentration in the range of 0.1 ng/mL ~ 1 mg/mL. The regression equation is $A = 3284.33 \times \lg C + 9497.26$, where C is the HRP concentration (ng/mL) and A is the Raman intensity at 1078 cm^{-1} ($R^2 = 0.9976$). The LOD calculated by 3 times the standard deviation rule (3S/N) was 0.053 ng/mL. Compared with the reported methods, this method has advantages for both linear range and LOD due to its advantages of high sensitivity and high specificity. Furthermore, the proposed strategy possesses low cost, and less time consumption (Table S3).

In addition, to verify the general applicability of our strategy in detecting other glycoproteins, ACP-imprinted MNPs and TRF-imprinted MNPs were prepared, with the imprinting times at 75 min and 70 min, respectively (Fig. S20). As shown in Fig. 5A, the ACP-imprinted MNPs exhibited a good linear response to ACP within the concentration range of 0.1 ng/mL~100 μg/mL ($A = 3912.13 \times \lg C + 9631.77$, $R^2 = 0.9892$). The TRF- imprinted MNPs exhibited a linear response toward TRF within the range of 0.01 ng/mL ~ 100 μg/mL ($A = 2875.12 \times \lg C + 9676.49$, $R^2 = 0.9924$, Fig. 5B).

3.7. Real sample analysis

To verify the feasibility of the SERS based on boronic acid affinity MMIPs recognition applied to real samples, this strategy was used for the detection of HRP in three spiked fetal bovine serum samples (1.0 ng/mL, 10 ng/mL and 100 ng/mL). The detection results of fetal bovine serum samples spiked with

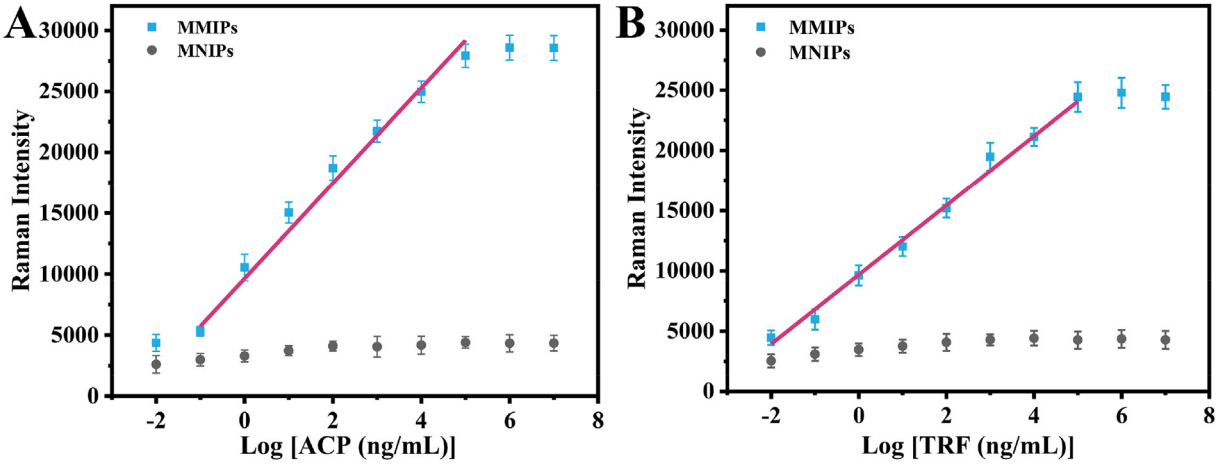

Fig. 5. (A) Calibration curve of SERS signal intensity at 1078 cm^{-1} for ACP at a concentration range of 0.1 ng/mL ~ 100 μg/mL. (B) Calibration curve of SERS signal intensity at 1078 cm^{-1} for TRF at a concentration range of 0.01 ng/mL ~ 100 μg/mL. Error bars indicate the standard deviation of three replicate determinations.

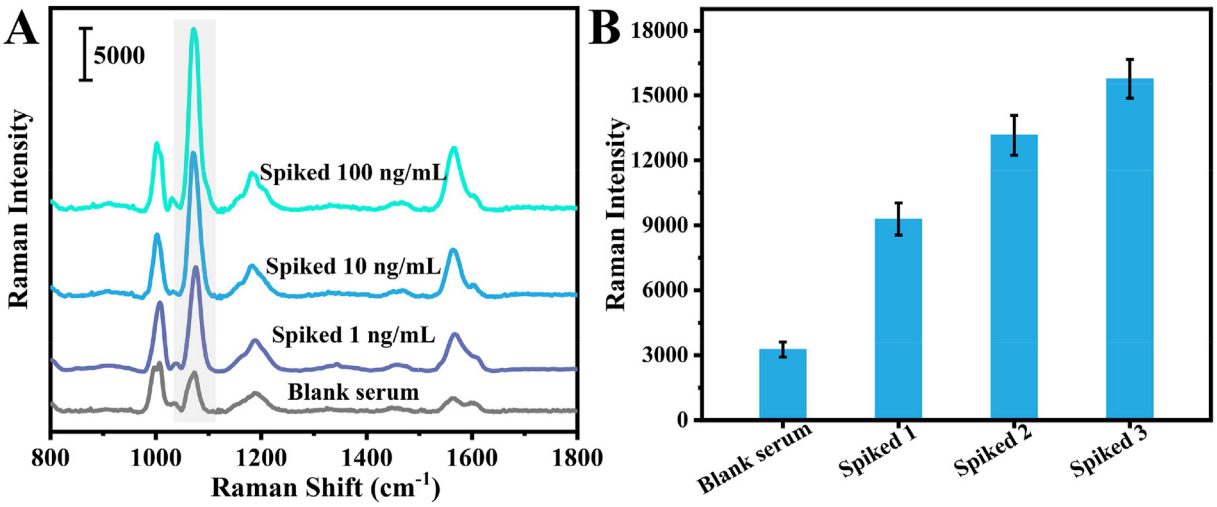

Fig. 6. (A) Raman spectra for serum samples spiked with different concentrations of HRP. (B)Raman intensities at 1078 cm^{-1} for serum samples spiked with different concentrations of HRP. Error bars indicate the standard deviation of three replicate determinations.

Table 1
Determination of HRP in fetal bovine serum samples (n = 3).

Spiked (ng/mL)	Detecte (ng/mL)	Recovery (%)	RSD (%)
0	/	/	/
1	0.9724	97.2	5.7
10	9.064	90.6	6.8
100	92.01	92.0	4.9

different concentrations of HRP are shown in Fig. 6. The recovery is at 90.6% ~ 97.2% with no more than 6.8% of RSD (Table 1). These results indicate that the proposed method can be used to detect target glycoproteins in real samples.

To assess universal applicability, the SERS sensor was also applied in the determination of ACP and TRF in non-spiked and spiked human serum samples (Table 2). The original concentrations of ACP and TRF are 1.651 ng/mL and 3.378 ng/mL, which are distributed within the normal ACP and TRF levels reported by former literature [43,49]. When the human serum samples spiked with ACP at 1.0 ng/mL, 5.0 ng/mL and 10 ng/mL, the recoveries are at 93.2% ~ 103.4%, and the RSD is no more than 7.0%. When spiked with TRF at 5.0 ng/mL, 10 ng/mL and 20 ng/mL, the recoveries are between 96.3% ~ 101.4%, and the RSD is no more than 7.3%. The concentrations of ACP and TRF in the above-mentioned samples were also quantified by commercial ELISA kit. There is no significant difference in accuracy and precision between the two approaches.

4. Conclusion

In summary, we combined boronate affinity MMIPs with boronate affinity-based SERS detection to propose a sandwich strategy to detect trace amounts of glycoproteins in biological samples. MMIPs containing boronic acid groups have nonimmune-biomimetic recognition of glycoproteins and high selectivity for target glycoproteins in serum samples. The prepared Au-MPBA@Ag had a high SERS activity, which was further modified with MPBA as SERS probes that could bind specifically to glycoproteins. Therefore, both selectivity and sensitivity of the sandwich strategy were guaranteed. The present method also has significant advantages in terms of cost-effectiveness, stability, and rapid detection. Furthermore, the method can detect other valuable glycoproteins by imprinting target glycoproteins such as ACP and TRF to be easily generalized to the detection of other glycoprotein biomarkers. This versatile strategy provides a non-destructive technique for clinical diagnostic applications. However, there were the low signal-to-noise ratio of MMIPs-based SERS due to the template leakage and residue. This makes the sensor less desirable for the detection of biological samples at very low concentrations. Therefore, the signal-to-noise ratio of this method need to be further investigated. It is noteworthy that using a portable Raman spectrometer in this study allows POCT and on-site applications. SERS as a sensitive technique, this strategy provides a new avenue for its biomimetic recognition in analysis, and it is foreseeable that this method has great potential in the diagnostic field and further applications in identifying other kinds of proteins have a promising prospect.

Table 2
Comparison of the precision and accuracy of SERS and commercial ELISA kit for the determination of ACP and TRF in serum samples (n = 3).

Sample	Added (ng/mL)	The proposed method			ELISA		
		Found (ng/mL)	Recovery (%)	RSD (%)	Found (ng/mL)	Recovery (%)	RSD (%)
ACP	0	1.651	/	6.8	1.870	/	5.1
	1.0	2.583	93.2	7.0	2.829	95.9	4.8
	5.0	6.716	101.3	6.3	6.982	102.2	3.7
	10.0	11.989	103.4	5.8	12.106	102.4	4.2
TRF	0	3.378	/	7.1	3.270	/	4.6
	5.0	8.238	97.2	7.3	8.483	102.1	5.2
	10.0	13.008	96.3	6.1	13.218	98.4	4.8
	20.0	23.658	101.4	6.9	24.238	104.3	5.7

CRediT authorship contribution statement

Cunming Hu: Conceptualization, Methodology, Writing – original draft, Investigation, Visualization, Validation, Data curation. **Fei Peng:** Validation, Data curation, Formal analysis. **Fang Mi:** Investigation, Formal analysis. **Ying Wang:** Data curation. **Pengfei Geng:** Investigation. **Lin Pang:** Investigation. **Yuhua Ma:** Supervision, Funding acquisition. **Guixin Li:** Funding acquisition. **Yingjun Li:** Writing – review & editing. **Ming Guan:** Conceptualization, Supervision, Project administration, Funding acquisition, Review & Editing the original and revised Draft.

Declaration of competing interest

The authors declare that they have no known competing financial interests or personal relationships that could have appeared to influence the work reported in this paper.

Acknowledgements

This work is supported by the National Natural Science Foundation of China (22064016, 52063028), Natural Science Foundation of Xinjiang Uygur Autonomous Region of China (2021D01A113, 2019D01A69, 2019D01B36), Xinjiang Uygur Autonomous Region University Scientific Research Program Key Project (XJEDU2019I019).

Appendix A. Supplementary data

Supplementary data to this article can be found online at https://doi.org/10.1016/j.aca.2021.339289.

References

[1] Pauline M. Rudd, Tim Elliott, Peter Cresswell, Ian A. Wilson, R.A. Dwek, Glycosylation and the immune system, Carbohydrates and Glycobiology 291 (2001) 2370–2376.
[2] C.L. Bonduelle, S. Lecommandoux, Synthetic glycopolypeptides as biomimetic analogues of natural glycoproteins, Biomacromolecules 14 (2013) 2973–2983.
[3] B.G. Ng, H.H. Freeze, Perspectives on glycosylation and its congenital disorders, Trends Genet. 34 (2018) 466–476.
[4] J. Sun, F. Yang, X.R. Yang, Synthesis of functionalized fluorescent gold nanoclusters for acid phosphatase sensing, Nanoscale 7 (2015) 16372–16380.
[5] J. Ge, J.H. Yu, H. Yang, D. Yang, R. Cai, Human serum albumin templated MnO2 nanosheets as an efficient biomimetic oxidase for biomolecule sensing, J. Mater. Chem. B 8 (2020) 11090–11095.
[6] L.P. Dong, S. Feng, S.S. Li, P.P. Song, J.D. Wang, Preparation of concanavalin A-chelating magnetic nanoparticles for selective enrichment of glycoproteins, Anal. Chem. 87 (2015) 6849–6853.
[7] F. Mi, M. Guan, C.M. Hu, F. Peng, S.J. Sun, X.M. Wang, Application of lectin-based biosensor technology in the detection of foodborne pathogenic bacteria: a review, Analyst 146 (2021) 429–443.
[8] J. Zhu, Z. Sun, K. Cheng, R. Chen, M.L. Ye, B. Xu, D. Sun, L.M. Wang, J. Liu, F.J. Wang, H.F. Zou, Comprehensive mapping of protein N-glycosylation in human liver by combining hydrophilic interaction chromatography and hydrazide chemistry, J. Proteome Res. 13 (2014) 1713–1721.
[9] W.T. Cong, A.Y. Zhou, Z.G. Liu, J.Y. Shen, X. Zhou, W.J. Ye, Z.X. Zhu, X. Zhu, J. Lin, L.T. Jin, Highly sensitive method for specific, brief, and economical detection of glycoproteins in sodium dodecyl sulfate-polyacrylamide gel electrophoresis by the synthesis of a new hydrazide derivative, Anal. Chem. 87 (2015) 1462–1465.
[10] J. Zhu, F.J. Wang, R. Chen, K. Cheng, B. Xu, Z.M. Guo, X.M. Liang, M.L. Ye, H.F. Zou, Centrifugation assisted microreactor enables facile integration of trypsin digestion, hydrophilic interaction chromatography enrichment, and on-column deglycosylation for rapid and sensitive N-glycoproteome analysis, Anal. Chem. 84 (2012) 5146–5153.
[11] Y. Tian, R.Z. Tang, L. Liu, Y. Yu, S. Ma, B.L. Gong, J.J. Ou, Glutathione-modified ordered mesoporous silicas for enrichment of N-linked glycopeptides by hydrophilic interaction chromatography, Talanta 217 (2020) 121082.
[12] Y. Yang, Y. Zeng, Microfluidic communicating vessel chip for expedited and automated immunomagnetic assays, Lab Chip 18 (2018) 3830–3839.
[13] D. Liu, F. Wu, Y. Cen, L. Ye, X.Y. Shi, Y.L. Huang, S.S. Fang, L. Ma, Comparative research on nucleocapsid and spike glycoprotein as the rapid immunodetection targets of COVID-19 and establishment of immunoassay strips, Mol. Immunol. 131 (2021) 6–12.
[14] S.S. Wang, W.Z. Li, P.W. Sun, Z.Q. Xu, Y.W. Ding, W.J. Xu, W. Xu, J. Gu, Selective extraction of myoglobin from human serum with antibody-biomimetic magnetic nanoparticles, Talanta 219 (2020) 121327.
[15] M.F. He, Y.M. Wei, R. Wang, C.Y. Wang, B. Zhang, L. Han, Boronate affinity magnetic nanoparticles with hyperbranched polymer brushes for the adsorption of cis-diol biomolecules, Microchimica Acta 186 (2019).
[16] X.X. Qin, Z. Zhang, H.J. Shao, R. Zhang, L.X. Chen, X.B. Yang, Boronate affinity material-based sensors for recognition and detection of glycoproteins, Analyst 145 (2020) 7511–7527.
[17] H.W. Zheng, H. Lin, X.F. Chen, J.J. Tian, T.R. Pavase, R.Q. Wang, J.X. Sui, L.M. Cao, Development of boronate affinity-based magnetic composites in biological analysis: advances and future prospects, Trac. Trends Anal. Chem. 129 (2020).
[18] Q. Yang, Y. Zhu, B. Luo, F. Lan, Y. Wu, Z.W. Gu, pH-Responsive magnetic nanospheres for the reversibly selective capture and release of glycoproteins, J. Mater. Chem. B 5 (2017) 1236–1245.
[19] Z. Liu, H. He, Synthesis and applications of boronate affinity materials: from class selectivity to biomimetic specificity, Acc. Chem. Res. 50 (2017) 2185–2193.
[20] C.C. Lu, H.Y. Li, H.Y. Wang, Z. Liu, Probing the interactions between boronic acids and cis-diol-containing biomolecules by affinity capillary electrophoresis, Anal. Chem. 85 (2013) 2361–2369.
[21] M. Dinc, C. Esen, B. Mizaikoff, Recent advances on core–shell magnetic molecularly imprinted polymers for biomacromolecules, Trac. Trends Anal. Chem. 114 (2019) 202–217.
[22] A. Yarman, S. Kurbanoglu, I. Zebger, F.W. Scheller, Simple and robust: the claims of protein sensing by molecularly imprinted polymers, Sensor. Actuator. B Chem. 330 (2021).
[23] J.F. Zhang, S.L. Li, Molecularly imprinted polymers-surface-enhanced Raman spectroscopy: state of the art and prospects, Int. J. Environ. Anal. Chem. (2020) 1–31.
[24] M. Arabi, A. Ostovan, A.R. Bagheri, X.Y. Guo, L. Wang, J. Li, X.Y. Wang, B.W. Li, L.G. Chen, Strategies of molecular imprinting-based solid-phase extraction prior to chromatographic analysis, Trac. Trends Anal. Chem. 128 (2020).
[25] E. Ekmen, M. Bilici, E. Turan, U. Tamer, A. Zengin, Surface molecularly-imprinted magnetic nanoparticles coupled with SERS sensing platform for selective detection of malachite green, Sensor. Actuator. B Chem. 325 (2020).
[26] Z.L. Chen, X.J. Liu, C.X. Huang, J. Li, X.T. Shen, Artificial cytochrome c mimics: graphene oxide-Fe(III) complex-coated molecularly imprinted colloidosomes for selective photoreduction of highly toxic pollutants, ACS Appl. Mater. Interfaces 12 (2020) 6615–6626.
[27] A.R. Cardoso, A.C. Marques, L. Santos, A.F. Carvalho, F.M. Costa, R. Martins, M.G.F. Sales, E. Fortunato, Molecularly-imprinted chloramphenicol sensor with laser-induced graphene electrodes, Biosens. Bioelectron. 124–125 (2019) 167–175.
[28] R.R. Xing, Y.Y. Ma, Y.J. Wang, Y.R. Wen, Z. Liu, Specific recognition of proteins and peptides via controllable oriented surface imprinting of boronate affinity-anchored epitopes, Chem. Sci. 10 (2019) 1831–1835.
[29] L.L. Zhou, Y.Y. Wang, R.R. Xing, J. Chen, J. Liu, W. Li, Z. Liu, Orthogonal dual molecularly imprinted polymer-based plasmonic immunosandwich assay: a double characteristic recognition strategy for specific detection of glycoproteins, Biosens. Bioelectron. 145 (2019) 111729.
[30] P. He, H. Zhu, Y. Ma, N. Liu, X. Niu, M. Wei, J. Pan, Rational design and fabrication of surface molecularly imprinted polymers based on multi-boronic acid sites for selective capture glycoproteins, Chem. Eng. J. 367 (2019) 55–63.
[31] J.F. Xie, G.Q. Zhong, C. Cai, C.Y. Chen, X.M. Chen, Rapid and efficient separation of glycoprotein using pH double-responsive imprinted magnetic microsphere, Talanta 169 (2017) 98–103.
[32] R.R. Xing, S.S. Wang, Z.J. Bie, H. He, Z. Liu, Preparation of molecularly imprinted polymers specific to glycoproteins, glycans and monosaccharides via boronate affinity controllable-oriented surface imprinting, Nat. Protoc. 12 (2017) 964–987.
[33] T. Zhou, M. Fan, R.Y. You, Y.D. Lu, L.Q. Huang, Y.C. Xu, S.Y. Feng, Y. Wu, H.Y. Shen, L.J. Zhu, Fabrication of Fe3O4/Au@ATP@Ag Nanorod sandwich structure for sensitive SERS quantitative detection of histamine, Anal. Chim. Acta 1104 (2020) 199–206.
[34] J.J. Du, C.Y. Jing, Preparation of thiol modified Fe3O4@Ag magnetic SERS probe for PAHs detection and identification, J. Phys. Chem. C 115 (2011) 17829–17835.
[35] J.J. Du, J.L. Cui, C.Y. Jing, Rapid in situ identification of arsenic species using a portable Fe3O4@Ag SERS sensor, Chem. Commun. 50 (2014) 347–349.
[36] C.M. Hu, L. Ma, F. Mi, M. Guan, C. Guo, F. Peng, S.J. Sun, X.M. Wang, T.W. Liu, J.T. Li, SERS-based immunoassay using core–shell nanotags and magnetic separation for rapid and sensitive detection of cTnI, New J. Chem. 45 (2021) 3088–3094.
[37] S.Y. Huang, J.Q. Xu, J.T. Zheng, F. Zhu, L.J. Xie, G.F. Ouyang, Synthesis and application of magnetic molecularly imprinted polymers in sample preparation, Anal. Bioanal. Chem. 410 (2018) 3991–4014.
[38] Y.Q. Shan, M.L. Wang, Z.L. Shi, M.L. Lei, X. Wang, F.-G. Wu, H.-H. Ran, G.M. Arumugam, Q.N. Cui, C.X. Xu, SERS-encoded nanocomposites for dual pathogen bioassay, J. Mater. Sci. Technol. 43 (2020) 161–167.
[39] S.S. Panikar, D. Cialla-May, E. De la Rosa, P. Salas, J. Popp, Towards translation of surface-enhanced Raman spectroscopy (SERS) to clinical practice: progress and trends, Trac. Trends Anal. Chem. 134 (2021).
[40] C.M. Hu, L. Ma, M. Guan, F. Mi, F. Peng, S.J. Sun, X.M. Wang, T.W. Liu, J.T. Li,

SERS-based magnetic immunoassay for simultaneous detection of cTnI and H-fabp using core-shell nanotags, Anal. Methods 12 (2020) 5442–5449.
[41] S.J. Sun, M. Guan, C. Guo, L. Ma, H. Zhou, X.M. Wang, F. Mi, J.T. Li, A novel surface-enhanced Raman scattering method for simultaneous detection of ketamine and amphetamine, RSC Adv. 10 (2020) 36609–36616.
[42] J. Ye, Y. Chen, Z. Liu, A boronate affinity sandwich assay: an appealing alternative to immunoassays for the determination of glycoproteins, Angew Chem. Int. Ed. Engl. 53 (2014) 10386–10389.
[43] X.X. Li, B.Z. Li, J.L. Hong, X. Zhou, Min, Highly selective determination of acid phosphatase in biological samples using a biomimetic recognition-based SERS sensor, Sensor. Actuator. B Chem. 276 (2018) 421–428.
[44] C.Y. Hong, X.X. Zhang, C.Y. Wu, Q. Chen, H.F. Yang, D. Yang, Z. Huang, R. Cai, W. Tan, On-site colorimetric detection of cholesterol based on polypyrrole nanoparticles, ACS Appl. Mater. Interfaces 12 (2020) 54426–54432.
[45] K.S. Yuan, Q.S. Mei, X. Guo, Y.W. Xu, D.T. Yang, Z.J. Jiang, H.B. Zhou, Antimicrobial peptide based magnetic recognition elements and Au@Ag-GO SERS tags with stable internal standards: a three in one biosensor for isolation, discrimination and killing of multiple bacteria in whole blood, Chem. Sci. 9 (2018) 8781.
[46] D.J. Li, Z.J. Bie, F.F. Wang, E.H. Guo, Efficient synthesis of riboflavin-imprinted magnetic nanoparticles by boronate affinity-based surface imprinting for the selective recognition of riboflavin, Analyst 143 (2018) 4936–4943.
[47] N. Li, J. Chen, Y.P. Shi, Magnetic polyethyleneimine functionalized reduced graphene oxide as a novel magnetic solid-phase extraction adsorbent for the determination of polar acidic herbicides in rice, Anal. Chim. Acta 949 (2017) 23–34.
[48] F.X. Gao, X.T. Ma, X.W. He, W.Y. Li, Y.K. Zhang, Smart surface imprinting polymer nanospheres for selective recognition and separation of glycoprotein, Colloids Surf., A 433 (2013) 191–199.
[49] Y.D. Zhang, Q.W. Huang, C. Ma, X.Y. Liu, H.X. Zhang, Magnetic fluorescent molecularly imprinted nanoparticles for detection and separation of transferrin in human serum, Talanta 188 (2018) 540–545.